Reviews

Interphase interaction in heterogeneous polymeric systems containing liquid-crystalline component

V. G. Kulichikhin, N. N. Avdeev, A. V. Semakov, and N. A. Platé**

A. V. Topchiev Institute of Petrochemical Synthesis, Russian Academy of Sciences, 29 Leninsky prosp., 117912 Moscow, Russian Federation. Fax: +7 (095) 230 2224

Some problems of analysis of interphase interactions in heterogeneous polymeric systems containing liquid-crystalline component are considered. Special attention is given to the methods of optical interferometry and dynamic mechanical spectrometry. The formation of interphase layers due to either partial compatibility or chemical interaction causes considerable improvement in mechanical properties of composite materials.

Key words: liquid-crystalline thermoplastic, interphase interaction; polymeric composites; optical interferometry and dynamic mechanical analysis.

Liquid-crystalline (LC) polymers, which retain a certain level of structural ordering in the liquid state, are no longer exotic. They became a generally recognized class of polymers, stimulating the development of new areas of fundamental science and solution of applied problems. Depending on the type of LC polymers there exist traditional areas, where their unique properties are realized. For the so-called comb-shaped polymers[1,2], macromolecules of which are built of flexible main chains (polyacrylate, polymethacrylate, polysiloxane, etc.) with rigid mesogenic groups linked through flexible spacers, these fields are electrooptics, electronics, and nonlinear optics. These applications are based on a tendency of the mesogenic groups of these polymers towards easy orientation and reorientation, and thus towards a sharp change in their optical properties in thin layers under the action of electric and magnetic fields of small intensity.

In the case of LC polymers[3,4], which contain mesogenic groups in the backbone, as well as in the case of macromolecules, which are composed of only mesogenic groups, engineering materials (high-strength fibers, plastics, and composites) are the most promising applications. In this case the ability of LC polymers to orient easily in mechanical fields, i.e., immediately during processing (flowing in spinning dies, extrusion dies, and injection molds) is used. Nevertheless, despite advantages of the anisotropic polymeric systems, their direct use is at present difficult because of the high cost of corresponding monomers and polymers. However, there exists an area where the practical use of linear LC polymers is possible just now. The case in point are the blended polymeric composites, which contain small amount of LC thermoplastics, and the systems with dispersed fillers. For mixtures two important effects are possible: a decrease in the viscosity of composites as compared to the thermoplastic, which is modified, and an improvement in its mechanical properties[5].

Both effects are due to the obvious reason, namely, the formation of thin low-viscous liquid threads by LC

Translated from *Izvestiya Akademii Nauk. Seriya Khimicheskaya,* No. 11, pp. 1862—1878, November, 1994.

1066-5285/94/4311-1753 $12.50

phase in the matrix of a commodity thermoplastic during processing, and their transformation into reinforcing high-strength fibers upon cooling of the molded sample. However, the judicious use of LC thermoplastics for modification of large-capacity polymers requires solution of a number of fundamental problems, which include: the achievement of high molecular orientation of LC phase, realization of a certain extent of its dispersion, choice of the type of distribution of LC phase over a cross-section (sometimes it is possible to attain migration of LC component on the surface of extrudates), and most important, to provide a sufficient interphase interaction. The latter factor is also extremely important for filled systems. Actually, the formation of heterophase structures is inevitably associated with the interphase interactions leading, eventually, to the appearance of a third phase, namely an interphase layer, which plays an important role in the processes of distribution of mechanical stresses under the conditions of deformation and change of the ratio between the elastic and dissipative components of the supplied energy.

The objective of this paper is to discuss some aspects of the role of interphase layers in modification of relaxation, rheological, and mechanical properties of polymeric composites. Our study is restricted to specific polymeric systems (as a rule, heterophase systems based on liquid-crystalline polyesters) and experimental techniques (mainly optical interferometry and mechanical spectroscopy, which are sometimes supplemented with the direct experimental techniques). In addition to generalization of the known experimental and theoretical data of the authors, this review presents original results published for the first time.

Principles now have been developed for the approach to the selection of blend components, making it possible to evaluate the affinity of polymers, at least, on an interface. One should bear in mind that despite the existence of compatible pairs of polymers (for example, polycarbonate—poly(methyl methacrylate)[6] it is very difficult to achieve complete compatibility in the melt under real-time conditions of the experiment because of low diffusion coefficients and limited thermal stability of polymers. In addition, mixing of polymers in the isotropic melt does not ensure compatibility of these polymers in the solid state because the phase and relaxation states of components change upon cooling, and cocrystallization or formation of solid solutions of one glassy component in the other one are highly improbable. Therefore, a system with incomplete decomposition to the different phases, which often shows high internal stresses, generally is realized in the solid state.

From the practical standpoint an ideal case would be a three-phase system: two phases of individual polymers and an interphase layer formed as a result of dosed diffusion, electron donor-acceptor interaction or a chemical reaction. In this case the coherence of phases of individual components would be assured. This is especially significant for the strains of blended and filled polymeric composites, such as bending, twisting, and compression.

The existing methods of analysis of interfaces at molecular level are briefly reviewed by Stamm[7]. For liquid components, in addition to conventional methods of evaluating the interfacial tension by the drop spreading method and measurement of the contact angle, the rotating drop procedure[8,9] and the breaking thread method[10,11] are presently quite popular.

According to the first procedure, a drop of one polymer (oligomer) is immersed in a higher density second polymer and the system is allowed to rotate. Due to the balance between centrifugal forces and interfacial tension, the shape of the rotating drop changes to cylindrical. The diameter of this drop is a measure of the interfacial tension. In the second case, the thread of one polymer is pressed into the matrix of another polymer, the system is converted to a melt state, and the kinetics of variation in geometry of the liquid thread controlled by interfacial tension is measured using a microscope.

For solid blends, the commonly used methods are spectral, based on scattering of electrons, neutrons, ions and their fragments, X-rays, IR radiation, and NMR using labeled nuclei, often using the variants of reflection; optical, electron, and scanning microscopy are employed as well. At most, these methods provide resolution up to 0.1—0.2 nm, i.e., allow one to analyze the elementary acts of interpenetrating fragments of diffusing macromolecules. It is natural that the conditions for using these methods are different for the free surfaces of blends (on the interface with air) and the so-called "hidden" interphase layers (between two polymers). In the latter case, specially prepared samples, generally in the form of sandwiches, are subjected to the action of nondestructive or destructive irradiations with subsequent analysis either of changes in characteristics due to interaction with the interface, or of the products of decomposition of labeled or nonlabeled components.

As an example, let us consider in detail one of the most simple and at the same time sufficiently informative method of interference microscopy (optical wedge), which allows registration of various stages of interdiffusion in melts of blends of oligomers and polymers.[12,13] The optical wedge method uses the interference of light passing through thin films of a polymer, where the interacting polymers are in side-by-side contact. Interference appears on the layer surface of the blend of liquid polymers, which fill the space of variable thickness ($40 < d < 150$ μm) between the glass plates with the semitransparent metal coating.

Since coherence is a necessary condition for interference of beams emerging from the point source, the used space should correspond to the operating wavelength of the light source. Thus, for irradiation of a

mercury lamp (λ = 546 nm) the space thickness should not exceed 300 μm, whereas for laser sources it may be increased to 500 μm and more. The interference picture (Fig. 1) is formed through interaction of the first two corresponding beams (passed without reflection and after undergoing a single reflection), with a path-length difference equal to

$$\Delta = 2dn + \lambda,$$

where n is the refraction index of the medium that fills the wedge. In the case of a homogeneous optical medium (n = const) the interference bands are the straight lines parallel to each other and to the edge of the wedge, the distance between the bands (pitch) being inversely proportional to the refraction index.

When the medium of an optical wedge is nonhomogeneous, i.e., $n = n(x,y)$, the interference bands naturally are not straight. At the initial moment of the experiment the boundary between the contacting components divides two systems of parallel interference bands with different pitches. Due to interaction of the components, gradients appear in their concentrations, leading in turn to a gradient in the refraction index, and as a result to distortion of the bands. The evolution of the bands with time provides information on distribution of component concentrations in the zone of diffusion and, thus, on the direction and rate of the diffusion stream. Specially obtained relationships between the refraction index and the concentration of solution of one component in the other one are used as the necessary supplementary data.

This method allows quantitative determination of coefficients of interdiffusion in the range from 10^{-9} to 10^{-15} $m^2 \cdot s^{-1}$. In addition, it may be used successfully to construct the phase diagrams of binary blends.[14] In this case the position of solubility curves on the concentration—temperature field is judged by the concentrations in the zone of diffusion near the interphase layer (this fact was previously verified for metal alloys)[15]. With a number of diffusion profiles at various temperatures, including the range of unlimited compatibility higher than the upper critical mixing temperature (UCMT) or below the low critical mixing temperature (LCMT), the phase diagrams are constructed (see, for example, Fig. 2).

For the pairs of polymers that form isotropic transparent melts, the applicability and usefulness of this method was demonstrated by its long-term use. However, if one of the interacting components is nontransparent in the visible region of the spectrum, as is observed for LC melts, the use of this method becomes conjectural because of incomplete information on diffusion concentration profiles. We are thus led to using modeling and additional methods. Thus, at a temperature above the isotropization point (T_i) of the LC component it is possible to study these systems, receiving information from both sides of the interface, whereas at $T < T_i$ only half the picture can be observed while registering dissolution of LC polymer in an isotropic thermoplastic. Then, taking the diffusion profile to be symmetric, the coefficients of interdiffusion can be estimated from the evolution of the interference

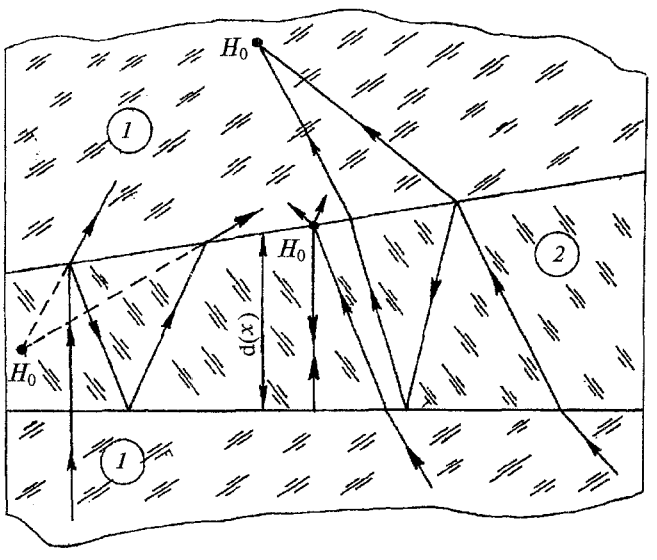

Fig. 1. Scheme of ray path in wedge space. *1*, glass plates; *2*, wedge space, filled with the studied polymer; $d(x)$, thickness of wedge at a distance x from the edge; H_0, points of localization of interference picture.

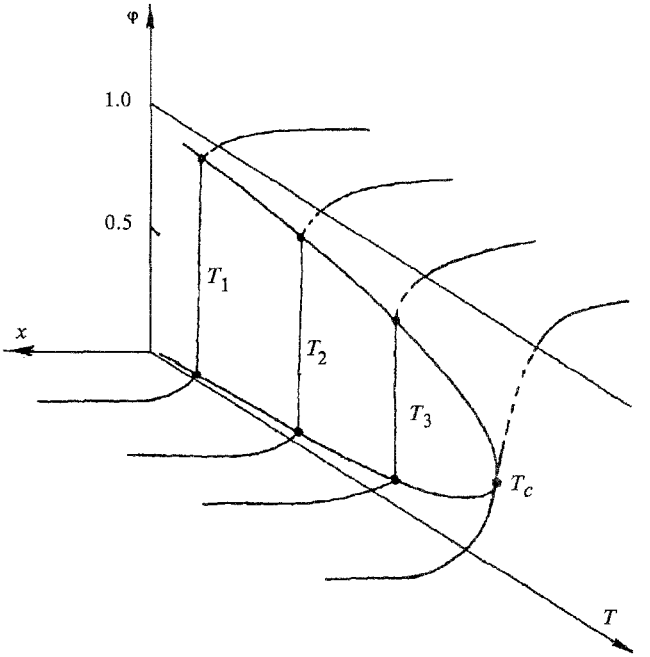

Fig. 2. Scheme of construction of phase diagram with UCMT from the data of optical interferometry at various temperatures. T_1, T_2, T_3 < UCMT; T_c = UCMT; φ, the volume fraction of component; x, coordinate of diffusion.

bands near the interface from the side of the transparent melt. The mixture poly(decamethyleneterephthaloyl-*bis*(4-oxybenzoate) (alkylenearomatic LC polyester) with poly(butylene terephthalate) (PBT) is a typical example of a system containing thermotropic LC polymer. Figure 3 presents the interferograms of the successive stages of developing the contact zone in the melts of the above polymers at sufficiently low rate of heating, along with the corresponding concentration curves.

In the initial state (Fig. 3, *a*) the system is nontransparent. At 230 °C PBT becomes clarified (melts) and the interference bands appear (Fig. 3, *b*). Bending of the bands near the interface suggests dissolution of polyester in PBT: a flat portion appears on the concentration curve, thus indicating partial compatibility of the components. In the polyester, the interference bands are not observed up to its transition to the isotropic state (295 °C). At $T > T_i$ the components are completely compatible and the composition monotonically varies from neat polyester to neat PBT (Fig. 3, *c*).

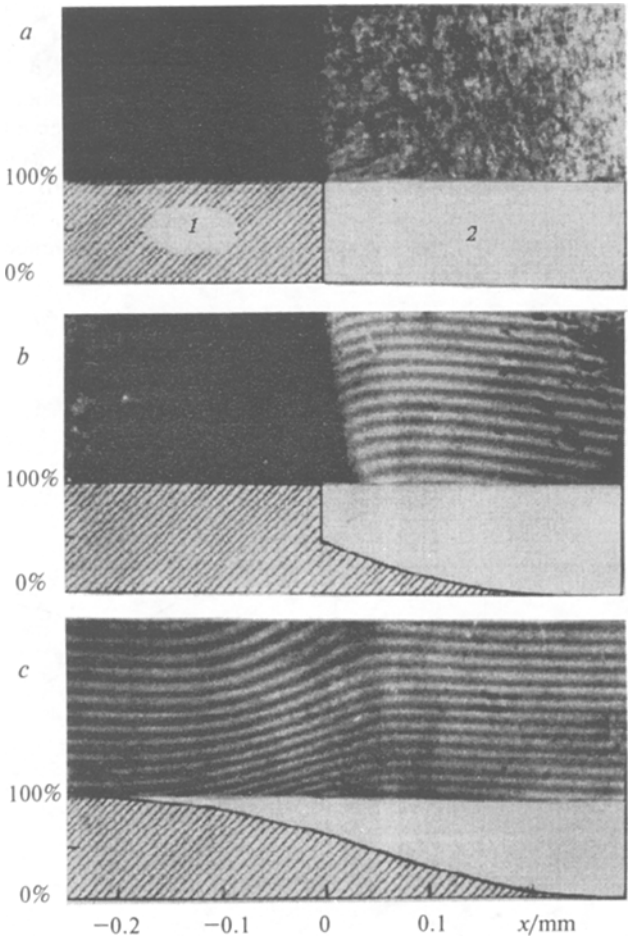

Fig. 3. Interferograms and concentration profiles of LC component for the system LC polyester (PES)—poly(butylene terephthalate) (PBT) at temperatures 100 (*a*), 230 (*b*), and 300 °C (*c*). *x* is coordinate of diffusion; *1*, PES; *2*, PBT.

Taking the limiting concentrations at the interface as solubilities of the components (this was justified above), we constructed the phase diagram of this system under heating (Fig. 4). It is characterized by the absence of amorphous decomposition to phases and superposition of two liquidus curves with eutectic point at $\varphi_{PBT} = 0.7$. This fact is confirmed by conservation of the transparent phase for the composition corresponding to eutectic upon cooling of the sample to 170 °C, i.e., to a temperature significantly below the crystallization temperatures of the components and solutions of different composition (Fig. 5). Upon heating, the eutectic zone first clarifies (at 215 °C), with the subsequent clarification of the zones of other compositions. In other words, upon heating, evolution of the interference pictures occurs in the reverse order.

The growth rate of the interphase layer caused by interdiffusion is sufficiently high for the polymers with these molecular masses (~50 000). In order to evaluate the growth rate of the interphase layer according to the second Fick's law, we calculated the interdiffusion coefficients D using the experimental profiles of concentrations.

$$\frac{\partial \varphi}{\partial t} = D \frac{\partial^2 \varphi}{\partial x^2}$$

(φ is the concentration, x is the coordinate of diffusion, t is the time of diffusion). Under initial and boundary

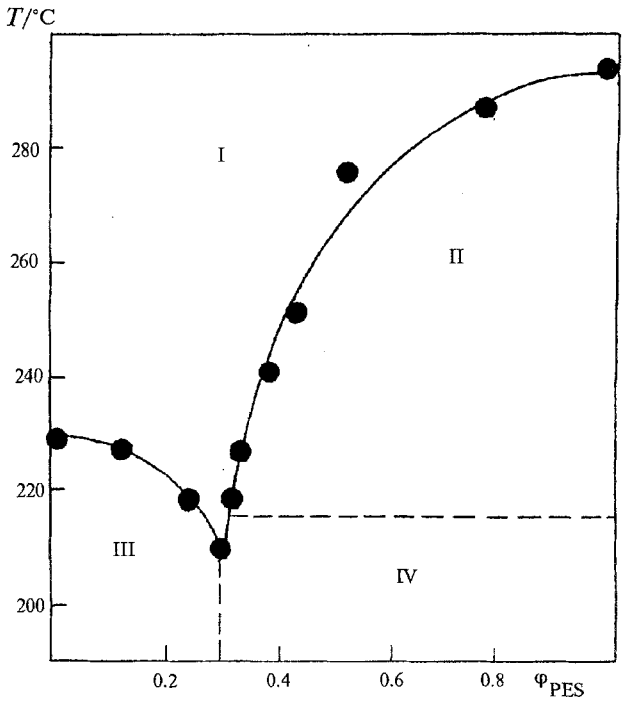

Fig. 4. Phase diagram for the system PES—PBT. I, region of isotropic solutions of variable compositions; II, LC state of PES; III, PBT in crystalline state; IV, PES in crystalline state.

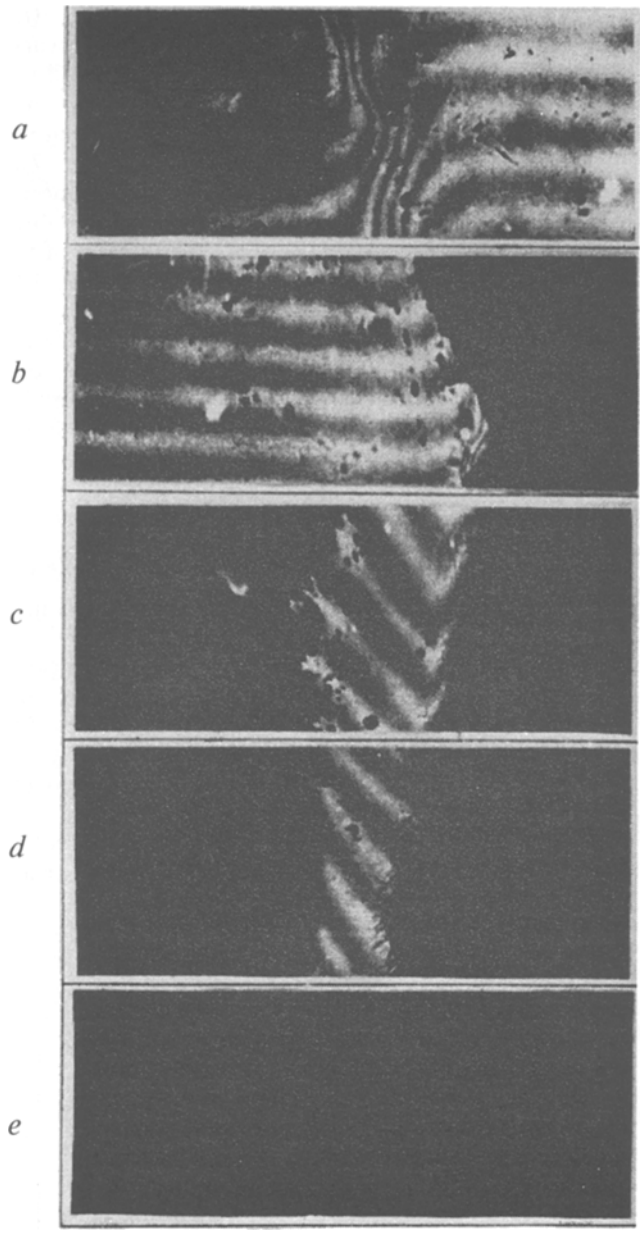

Fig. 5. Evolution of intensity of illumination of field of vision upon cooling of the mixture PES—PBT: T/°C: ~310 (*a*), 270 (*b*; PES crystallizes), 220 (*c*, PBT crystallizes), 210 (*d*; the eutectic zone is lighted up) and 20 (*e*).

conditions (in the case of contact of two semi-infinite media)

$$\varphi(x,0) = \begin{cases} 1; x < 0 \\ 0; x > 0 \end{cases} \qquad \varphi(x,t) = \begin{cases} 1; x = -\infty \\ 0; x = +\infty \end{cases}$$

we obtain[16]:

$$\varphi = 1/2\ (1-\mathrm{erf}\ U)$$

where $U = x/2$; erf U is the Gauss error integral.

To simplify the calculations we used a probability diagram (Fig. 6). At $T < T_i$ the interdiffusion coefficients D are 10^{-13} $m^2 \cdot s^{-1}$, whereas at $T > T_i$ these coefficients are higher by one order of magnitude, 10^{-12} $m^2 \cdot s^{-1}$.

Although this method is universal it is difficult to use it for the systems containing LC components because of some ambiguity of the results. While for the mixture of isotropic polymers orientation of macromolecules on the interface is of no importance, in the case of LC component the preferable molecular orientation on the interface plays an important role.

Depending on orientation of molecules (along or across the interface), the diffusion properties may differ. Therefore, in spite of the fact that the affinity (in this case the chemical similarity) of the components is the driving force of the process, the quantitative characteristics of diffusion for one and the same mesophase polymer may be different. In other words, the above-mentioned approach is the first attempt to make at least a rough estimation of the compatibility of a pair of polymers, of which one is a liquid-crystalline polymer. It is suggested that this approach will be further developed taking into account certain orientation of LC polymers in the contact zone.

The optical method allows for the direct observation of interdiffusion (solubility) of the components in the early stages. However, this method does not provide the answer to the main problem on the dissipation of the supplied mechanical energy over interphase layers. The answer to this problem can be obtained using dynamic

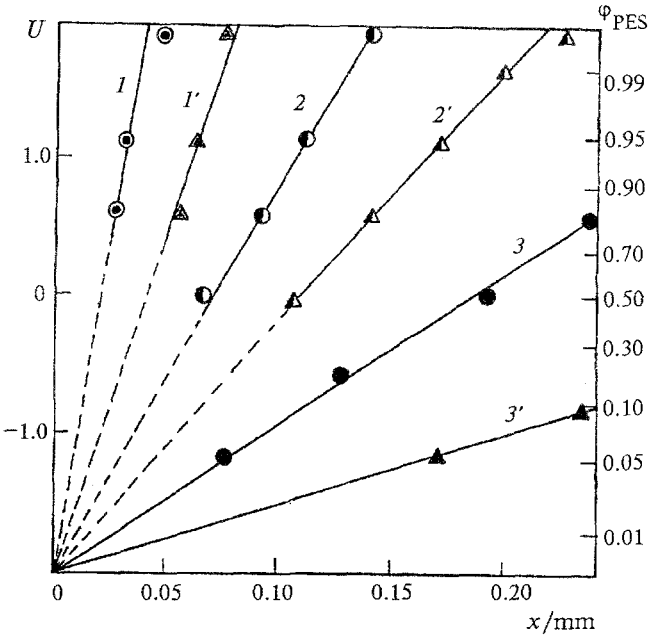

Fig. 6. Concentration curves (PES—PBT) plotted on the probability diagram for various diffusion times (*1*, *2*, *3*, 30 min; *1'*, *2'*, *3'*, 60 min) and temperatures (*1*, *1'*, 210 °C; *2*,*2'*, 270 °C; *3*, *3'*, 310 °C).

mechanical analysis, which complements well the optical method. In the case of dynamic mechanical spectroscopy, the system is subjected to the action of low-amplitude vibrations. For a pure elastic (Hooke's) system, the supplied energy completely reenters each cycle (phase difference between the sinusoids of strain and stress is 90°). For a neat viscous liquid, all the supplied energy dissipates into viscous friction (no phase difference between the corresponding sinusoids). For the viscoelastic polymeric system, a part of the supplied energy elastically recovers in each cycle (this part is characterized by elastic modulus E'), whereas the other part dissipatively scatters in the material (characterized by loss modulus E''). The ratio between these two moduli (mechanical loss tangent tan δ) "feels" the appearance of new relaxation regions in the system (interphase layers). Using mechanical spectroscopy we get the gross-characteristics sensitive to the variation in structure and phase state of the material. This method is applicable both for the melts of polymer blends and for solid blended and filled composites.

In the case of melts of incompatible polymers, the relaxation spectra can be used for quantitative evaluation of interfacial tension.[17] It is assumed that additional losses appear in a heterogeneous system as a result of tension between the drops of a disperse phase and a matrix. Then the complex elastic modulus of the blend is calculated as

$$E^*=\varphi E^*_1+(1-\varphi)E^*_2+E^*_I$$

where $E^*_i = E_i' + E_i''$, E^*_i are the complex elastic moduli of the i-th component; E^*_I is the contribution of interfacial tension to the complex modulus.

This indicates that in the relaxation spectrum $H(t)$ of the mixture, an additional area of relaxation appears due to the presence of interface rather than the additive summaring of the corresponding contributions of the neat polymers. This approach was verified for the mixture polystyrene—poly(methyl methacrylate) (Fig. 7). It was shown that the additional relaxation with time τ_I is caused by the interfacial tension. Moreover, its value was calculated.[17] For the given mixture it turned out to be 2.2 x 10^{-3} N/m, which is close to the value determined by other methods.

We attempted to use this approach for the melts of blends of aromatic polysulfone (PSF) based on dichlorodiphenylsulfone and diphenylolpropane and liquid-crystalline copolyester (CPE) Ultrax KR 4002 (BASF, Germany), which contains units of dioxydiphenyl, terephthalic and isophthalic acids, using the frequency dependence of mechanical loss tangent (Fig. 8). In this case we also succeeded in finding the additional relaxation area with a relaxation time of ~10 s, which appears in the spectrum of the blend and is not observed in the spectra of the neat components. However, the profile of the peak turns out to be broader than for the previous pair. This may be considered an indication of the presence of interphase interaction in this system.

To analyze this interaction we used the method of constructing three-dimensional dependences (dynamic modulus—blend composition—temperature) for solid composites to observe the position of relaxation transitions of the starting components[18]. These dependences for elastic modulus and loss modulus are given in Fig. 9

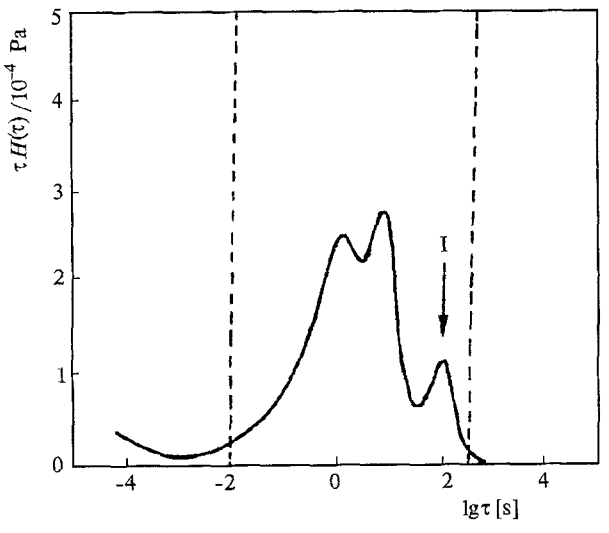

Fig. 7. Relaxation spectrum of the system PS—PMAA. Asterisk shows the additional relaxation time appearing due to the formation of interphase layer.

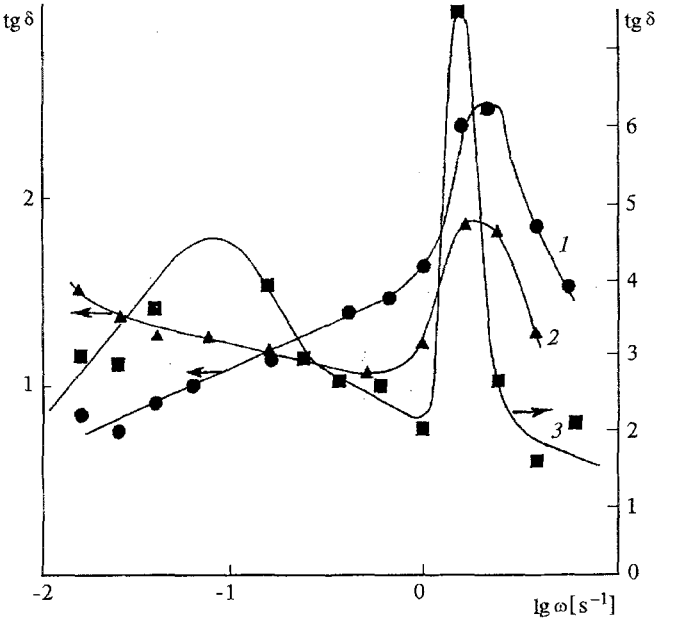

Fig. 8. Dependence of mechanical loss tangent on frequency (ω) for PSF (*1*), LC copolyester Ultrax (*2*) and their 50 : 50 blend (*3*).

(*a* and *b*). In the studied range of temperatures each component of the mixture shows two regions of molecular relaxation: low-temperature defreezing of fragmental mobility (γ-relaxation) and glass transition (α-process). Thus, for amorphous PSF the glass transition temperature T_g is 184 °C, whereas for partially crystalline at these temperatures PSF T_g = 122 °C. The temperatures of the maxima of γ-processes in PSF and CPE are 87 and 35 °C, respectively. Over the entire interval of the blend compositions, separate glass transitions of the components are observed. At first sight this argues for their thermodynamic incompatibility. However, more detailed information on the effect of the second component on the position of relaxation transitions can be obtained from the loss modulus isolines map (Fig. 10).

It is important to note the following: both for α- and γ-transitions the loss maxima are observed at certain concentration of CPE (10—20 and 80—90 %), and the temperatures of transitions change somewhat depending on composition. The method of mechanical spectroscopy is especially sensitive to relaxation transitions in the polymers of different nature and can trap the drift of glass transition point in the 1—2 °C range. For rigid chain polymers and their blends, the DSC technique is less informative for these purposes.

Let consider in more detail the role of the second component in the main relaxation process without discussing the tendencies in the variation of positions of γ-transitions.

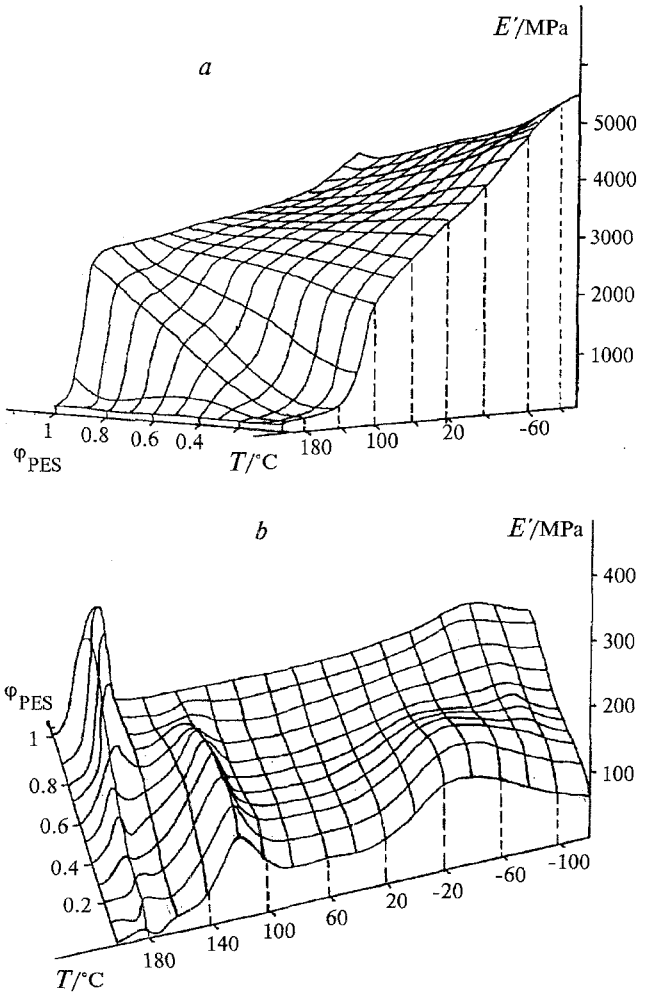

Fig. 9. Three-dimensional dependences of elastic modulus (*a*) and loss modulus (*b*) on concentration (φ) and temperature.

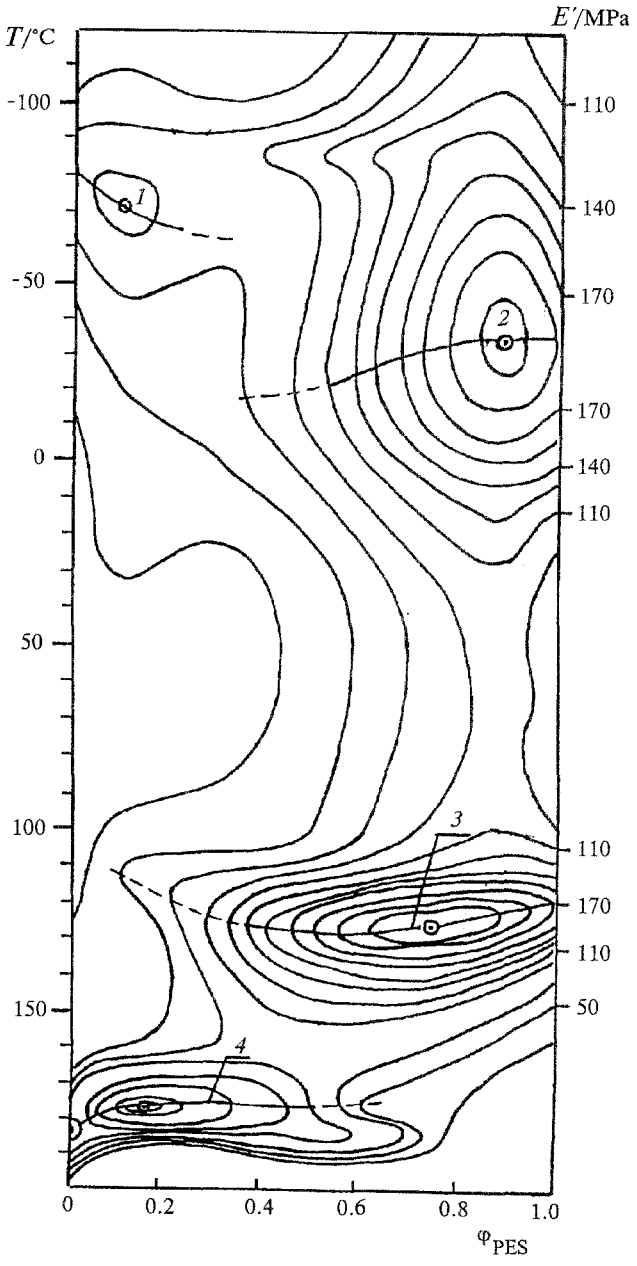

Fig. 10. Loss modulus isolines map for the blends LC copolyester Ultrax (PES-1) and polysulfone (PSF) of various compositions at different temperatures. T_α and T_γ are the points of α- and γ-transitions. *1*, T_γ PSF; *2*, T_γ PES-1; *3*, T_α PES-1, *4*, T_α PSF.

The presented data clearly shows a small increase in T_g of CPE upon adding ~22% PSF and, on the contrary, a marked decrease in T_g of PSF after adding CPE. Incidentally, in this region of the map two loss maxima are observed, one of which corresponds to 100% PSF, whereas the second maximum is located at 15% CPE. This suggests, first, the distribution of PSF macromolecules by relaxation properties in the presence of CPE and, second, the effect of morphology on dissipation of mechanical energy.

Earlier,[19] we described the morphology of blended extrudates obtained using a capillary viscometer. Upon addition of CPE in PSF, the anisodiametric structures of CPE (due to extension of the spherical drops in the zone of entrance into capillary) appear already at 5% of CPE, whereas at 15% concentration they transform to continuous thin threads 1—10 μm in diameter (Fig. 11). At 20—30% of CPE the continuous LC skin of the extrudate is formed and separate threads begin to get together into layers. In the range of 50—60% CPE the phase inversion takes place and CPE becomes a matrix, where the rigid inclusions of PSF are distributed, not necessarily of anisodiametric form. Stretching of the PSF drops into threads becomes appreciable at ~80% of CPE.

Thus, the positions of loss maxima reflect the maximum dispersity of the structure of the composite, when the maximum effect of the neighbor is observed, i.e., the peculiar state of the system near interfaces. Leaving for the future the quantitative description of the observed changes of T_g of the components in the blends of PSF with CPE in terms of the generally adopted theoretical views, we can state that as PSF is added to the CPE matrix (right side of the map), T_g first grows (up to C_{PSF} ~24%) and then gradually decreases. Recall that the specific surface of the dispersed phase changes in much the same fashion. This suggests that the change in T_g of CPE is associated with the interphase interaction of the components, which is maximal in the region of highest dispersity of the heterogeneous phase. The interaction of CPE macromolecules with more rigid phase structures of PSF leads to restriction of their mobility and, as a result, to an increase in rigidity.

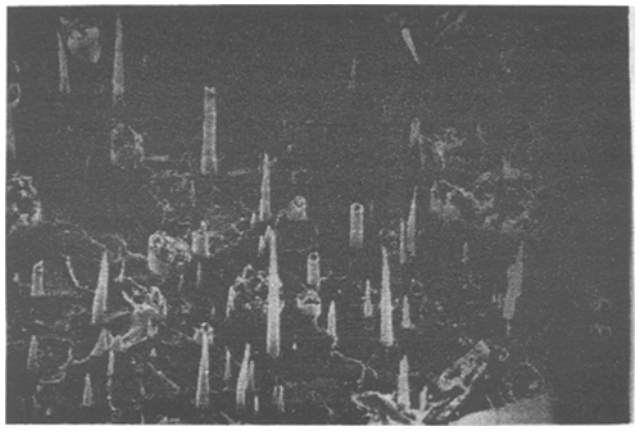

Fig. 11. Morphology of blend extrudate at 10% content of LC component (white fibers).

In the left portion of the map the situation is different. Small additives of CPE (3—10%) sharply decrease the glass transition temperature of PSF. The effect reaches 6—8 °C. In this case for neat PSF the loss maximum remains unchanged. It seems likely that, in addition to the developed morphology of the system, in this region of compositions we should allow for the plasticization effect of CPE with respect to PSF due to interdiffusion of macromolecules of the components. The presence of phenyl groups in the studied polymers allows us to expect a tendency of similar-to-similar attraction, although we cannot exclude intermolecular bonding between methyl groups of PSF and oxygen of carbonyl groups of CPE. This conclusion is supported by an increase in the temperatures of γ-transitions for both components in the presence of each other. A decrease in the local mobility of molecular fragments under conditions when these bonds are formed is highly probable.

Presentation of relaxation processes in the blends as loss modulus isolines maps allows one to judge the shift of temperatures of relaxation processes. However, it is possible to make a more through analysis of superposition of relaxation processes in polymeric systems using a theoretical approach to constructing these maps. This approach was developed[20] for the blend of linear high-molecular-mass polyethylene (PE) and mesophase poly-*bis*(trifluoroethoxyphosphazene) (PF) containing no mesogenic groups, but forming a state intermediate between the crystalline and isotropic states with one-dimensional positional order in the range of 80—250 °C.

Figure 12 presents dependences of elastic modulus E'(*a*) and loss modulus E'' (*b*) on composition (φ) and temperature (T). As is seen, the viscoelastic properties of the blends inherit the properties of the starting components and are controlled first of all by the molecular processes taking place in PE and PF. For the starting high-molecular-mass PE, three regions of molecular relaxation are seen, with the position of maxima E'' at −103 (I), 7 (II), 78 °C (III), along with the process of melting at 137 °C (IV). In regions I and II molecular motion can be ascribed to quasi-independent and cooperative motion of segments of the chain comparable with the Kuhn segment, i.e., it corresponds to γ- and α-processes in amorphous polymers, respectively. In region III the process of molecular relaxation is usually associated with the motion of molecular chains in amorphous PE regions near the interface with crystallites.[21]

The other component of the blend, PF, shows two regions of molecular relaxation: at −160 (I) and −39...−7°C (II). In region I relaxation is apparently caused by the local mobility of PF chains in an amor-

phous portion and is weakly expressed. The glass transition of PF depends significantly on the phase structure, and under conditions of high crystallinity (80—90%) it turns out to be blurred, occurring over a wide temperature interval. Therefore, it was suggested[22] that various types of disordered regions, which differ in conformation of macromolecules, exist in the amorphous fraction of PF. At 82 °C (III) the crystalline phase—mesophase transition occurs. Thus, in this temperature interval the blended compositions of PE and PF should inherit five relaxation processes and two phase transitions.

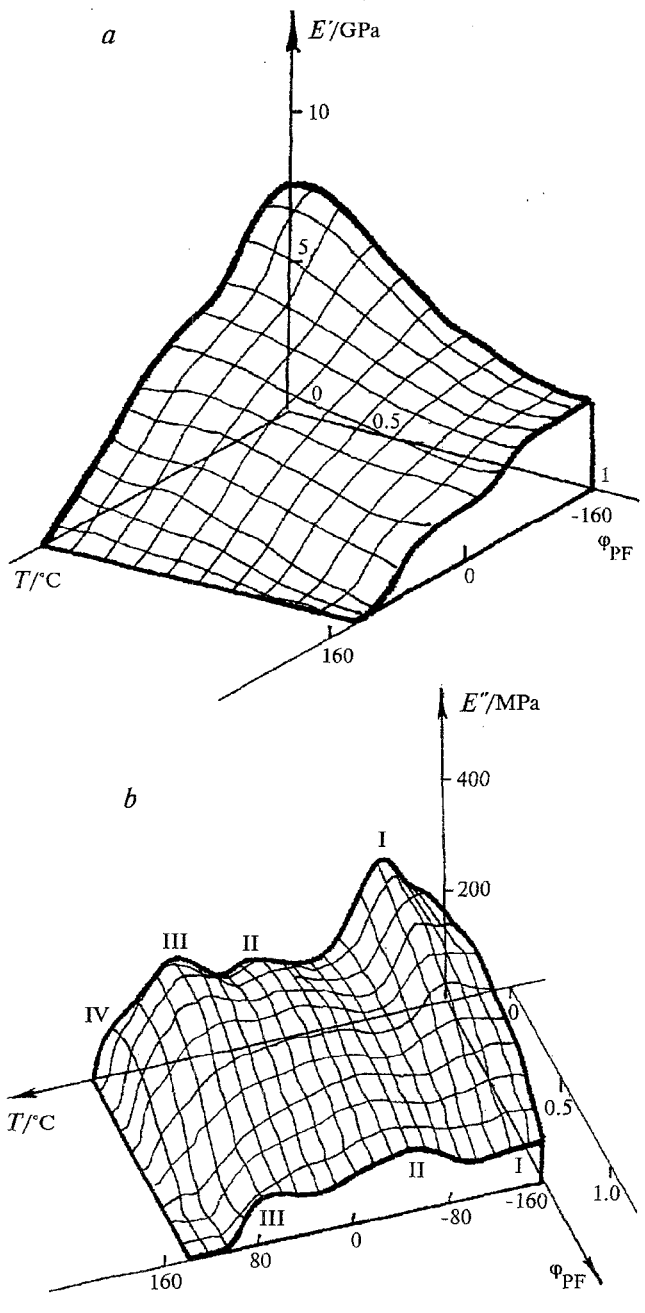

Fig. 12. Dependences of elastic modulus of (*a*) and loss modulus (*b*) on composition of the blend polyethylene (PE)—poly-*bis*(trifluoroethoxyphosphazene (PF) on temperature. *I*, *II*, *III*, and *IV* are the positions of maxima E'' for three regions of molecular relaxation and melting at 137 °C.

Superposition of various relaxation and phase transitions can be demonstrated more clearly using the above-mentioned maps of dissipative losses. Figure 13, *a* presents the experimental map of loss modulus $E''(\varphi, T) = \text{const}$ for the blend, whereas Fig. 13, *b* is the calculated isoline map E'' of the upper value of the loss modulus (parallel two-component model of deformation, which provides for simultaneous extension of morphological structures of two components[20]). Their comparison shows that over the entire temperature interval the experimental values of the loss modulus of compositions turn out to be higher than the upper possible estimates. This means that in terms of these model views it is impossible to reproduce correctly the E'' values of the blends, to say nothing of the peculiarities of their relaxation processes.

It seems reasonable to suggest that an interface or an intermediate layer is the source of additional dissipation of mechanical energy in blends. Molecular processes occurring in this layer determine the mechanism of dissipation of elastic energy on the interface.

By analogy with the complex elastic modulus let us consider for polymer melts the possibility for describing the dissipative properties of PE and PF blends in the solid state using a three-component addition scheme

$$E'' = \varphi_{PE}E''_{PE} + \varphi_{PF}E''_{PF} + \varphi_l E''_l ,$$

where φ_l is the volume fraction of the layer and E''_l is the loss modulus of transition layer. Then we believe that the loss modulus of the layer E''_l is the function of only temperature, and the volume fraction of the layer in the blend φ_l is the function of only composition of the blend

$$E''_l(\varphi, T) = E''_l(T),$$

$$\varphi_l = \varphi_{max}\,\phi(\varphi).$$

Here $\varphi_{max}E''_l(T)$ is the maximum value of the volume fraction of the transition layer in the blend achieved upon a change in its composition; $\phi(\varphi)$ is the ratio of volume of the transition layer at a given concentration to its limiting value, φ_l/φ_{max}.

Taking into account the above assumptions, the contribution of the layer to the overall losses of the blend (function of two variables) can be presented as the product of functions of one variable

$$\varphi_l E''_l = \phi\,\varphi_{max}\,E''_l(T)$$

where $\varphi_{max}E''_l(T)$ is the maximum contribution of the interphase layer to the losses.

Figure 13, *c* shows the isoline map of the excess of experimentally determined values of the loss modulus

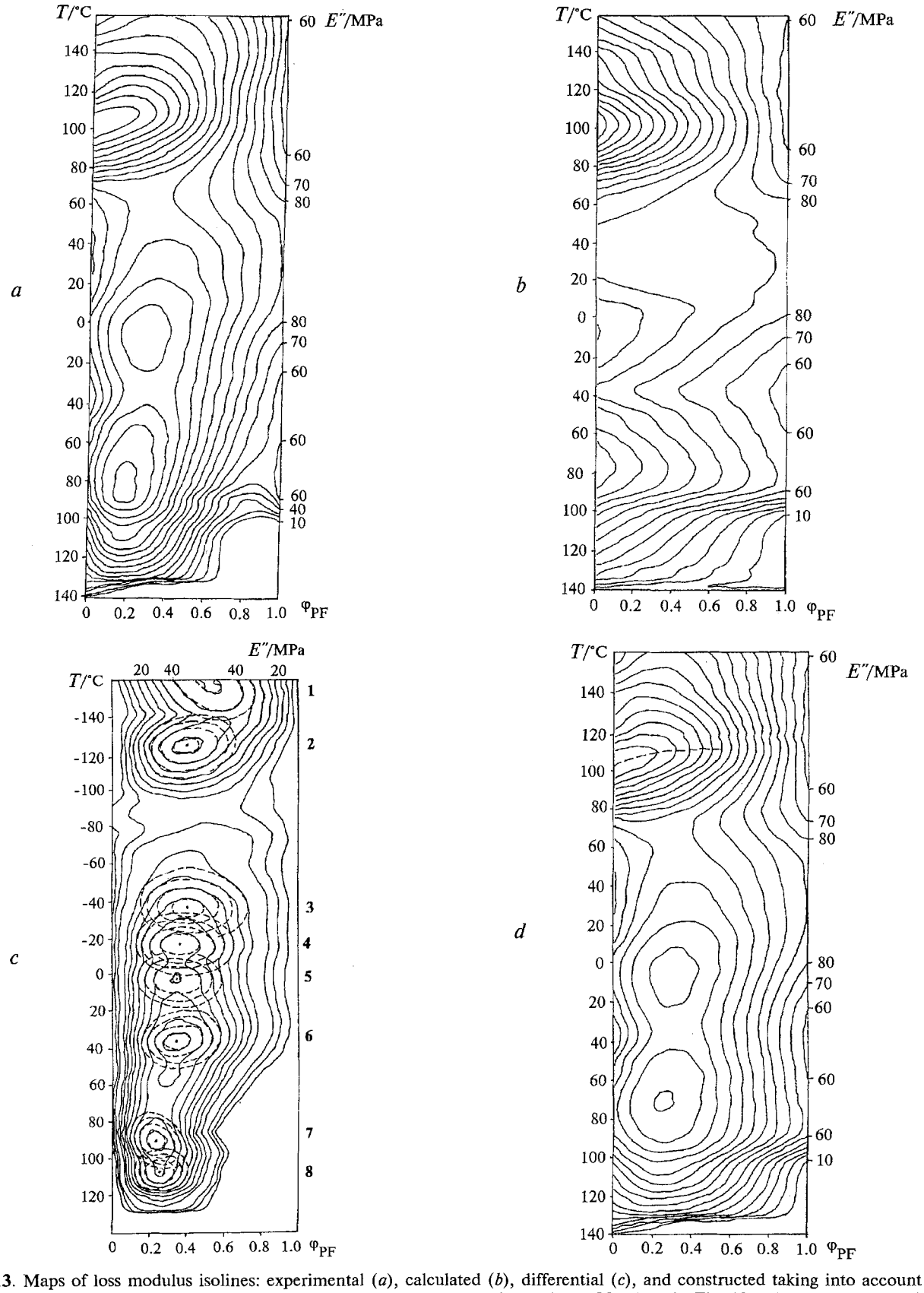

Fig. 13. Maps of loss modulus isolines: experimental (*a*), calculated (*b*), differential (*c*), and constructed taking into account the interphase layer (*d*). Broken lines reflect the unit relaxation processes in the layer. Numbers in Fig. 13 *c* show dispersions of loss modulus corresponding to different transitions at −160(*1*), −122(*2*), −34(*3*), −14(*4*), 4(*5*), 37(*6*), 92(*7*), and 108 °C (*8*).

of the blend compared to the values calculated according to the additive model and taking into account the fact that the volume fraction of the layer is small

$$\varphi_l << \varphi_{PE} + \varphi_{PF}.$$

In fact, the map in Fig. 13, *c* is the difference between maps *a* and *b*, i.e., it shows the additional losses $\varphi_l E_l''$ caused by the presence of the interphase layer. The maximum contribution of the layer to the losses $\varphi_{max} E_l''(T)$ is observed at 20—35% content of PF. This is not surprising, because it is at this concentration of the second component that a virtually defectless fiber system of the disperse PF phase in the PE matrix is formed during extrusion, which works according to the parallel scheme of deformation under external loading. In fact, this value is the loss modulus in the transition layer calculated with the accuracy of the numeral coefficient (maximum volume fraction of the transition layer).

With these data, we can construct the real map of modulus isolines for the three-phase model. For this purpose it is necessary to know the variation of E_l'' in terms of temperature and composition of the blend. The temperature dependence of the contribution of the interphase layer to losses determined for the above-mentioned interval of compositions is given in Fig. 14. The composition dependence of the volume fraction of the layer standardized by the maximum value of φ/φ_{max} can be determined from the temperature cross-section of the dependence $E_l''(\varphi, T)$ at T = const (in this case −122 °C). This dependence determined for γ-relaxation in PE is plotted in Fig. 15.

Using the values of ϕ and $\varphi_{max} E_l''(T)$, we reconstructed the modulus isoline map, which takes into account the existence of the transition layer (Fig. 13, *d*). Comparison with Fig. 13, *a* shows that the reconstructed map agrees well with the experimental map of losses (Fig. 13, *a*). Thus, the observed dissipation of the mechanical energy in the blends of PE and PF can be adequately described in terms of the three-component additive model. A nontrivial result of this approach is the possibility for multiplicative representation of the loss function in the layer. This, in turn, means that the layer, in addition to the neat components, can be characterized by its relaxation time spectrum, which remains essentially constant with changes in the blend composition.

From the viewpoint of the physical chemistry of polymers, it is of great interest to reveal and identify the relaxation processes in the transition layer (Fig. 13, *c*). For this purpose, it is necessary to be aware of the effect of temperature on the molecular processes in the transition layer and in the PE and PF volumes. This necessitates separation of superimposing processes. The modulus—composition—temperature diagram presents the unit relaxation processes in the layer as a set of embedded levels of elliptic shape (dashed lines in Fig. 13, *c*). The suggested procedure allows one to reveal in an interphase layer eight dispersions of loss modulus, which correspond to different relaxation and phase transitions with temperatures, °C: −160(*1*), −122(*2*), −34(*3*), −14(*4*), 4(*5*), 37(*6*), 92(*7*), and 108(*8*). Using the concept about the inheritability of the properties of the layer (in fact, this indicates correspondence between the transition temperatures in the layer, PE, and PF) these mentioned processes can be identified as follows. Processes *1* and *2* are caused by the quasi-independent small-scale motion of PE and PF segments, respectively (γ-relaxation). Processes *3* and *4* reflect cooperative movement of PF fragments (α-relaxation of PF molecules). Process *5* is attributed to the cooperative movement of PE segments (α-relaxation of PE molecules). Processes *6* and *8* correspond to the molecular motion of PE molecules in the near crystalline regions (α'- and α"-relaxation of PE molecules).

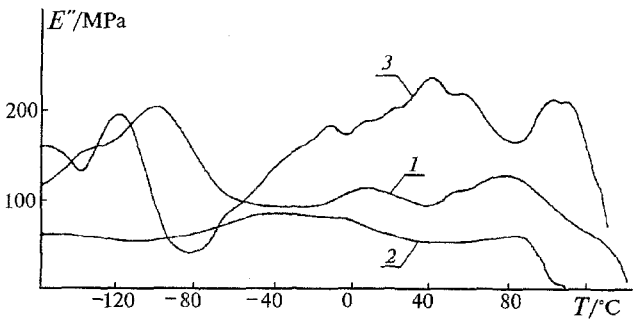

Fig. 14. Temperature cross-sections of three-dimensional modulus—composition—temperature dependences given in Fig. 12 *b* for PE (*1*), PF (*2*), and interphase layer at 30% content of PF (*3*).

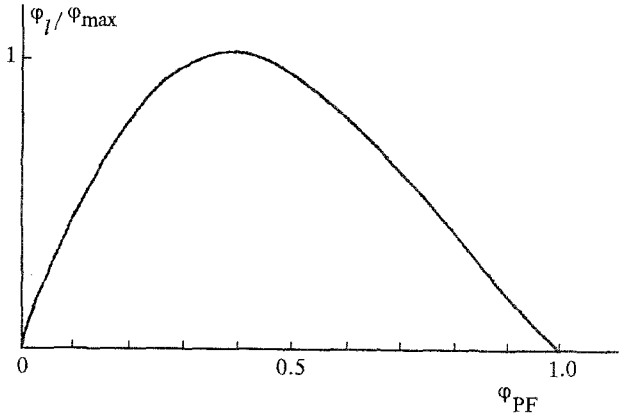

Fig. 15. Relative fraction of the interphase layer for PE—PF blends of various compositions.

Scheme 1

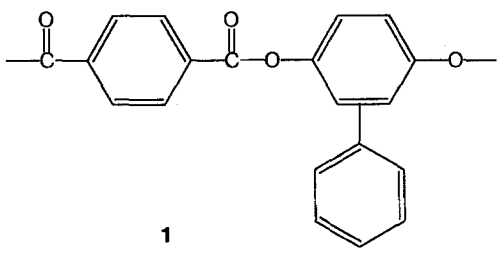

1

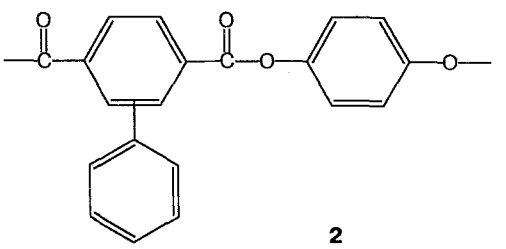

2

And last, process 7 indicates the mesomorphous PF transition in blends.

Comparison with the corresponding temperature transitions in individual polymers demonstrates a significant decrease in the low-temperature transitions (for example, γ-relaxation of PE in blend occurs at a temperature 19 °C less than in the neat PE), glass transition of PE in the interphase layer is observed at a temperature 3 °C less than in neat PE. This means that the stress fields on the interface affect the fragmental mobility of the chains to a more marked extent than the segmental (large-scale) mobility.

The glass transition of PF in the interphase layer is divided into two stages and shifted toward the region of low temperatures by 7 °C. This may be caused by the difference in relaxation characteristics of PF macromolecules near and far beyond interfaces.

Mesomorphic transition of PF in blends occurs at a higher temperature than in individual PF. From the thermodynamic viewpoint this should mean compression of PF in the PE matrix; the magnitude of internal pressure can be estimated from the shift of the transition temperature using the Clapeyron—Clausius equation.

Thus, separation of dissipative properties of the interphase layer in terms of the three-component model of the blend and subsequent separation of molecular processes in the layer is a sufficiently informative method, allowing us to judge the character of interphase processes in heterogeneous polymer systems.

For blended composites the formation of interphase layer or, in other words, partial compatibility of the components is important. Therefore, when choosing the particular pair of the modifying and modified polymer, components with similar functional groups are used to provide interaction according to a tendency of similar-to-similar attraction. The development of this principle brought us to the idea of mixing two LC polyesters of the following structure (Scheme 1).

Actually, if LC polymer can be even partially compatible with any other polymer, then the best partner would be also the LC polymer, which exists in the melt in the same nematic state. To put it another way, in addition to the similarity of the chemical structure of the chain, in this case the principle of identity of the phase states for the mixing components is also observed. The comparison of the dissipative properties of the mechanical blends was performed according to the

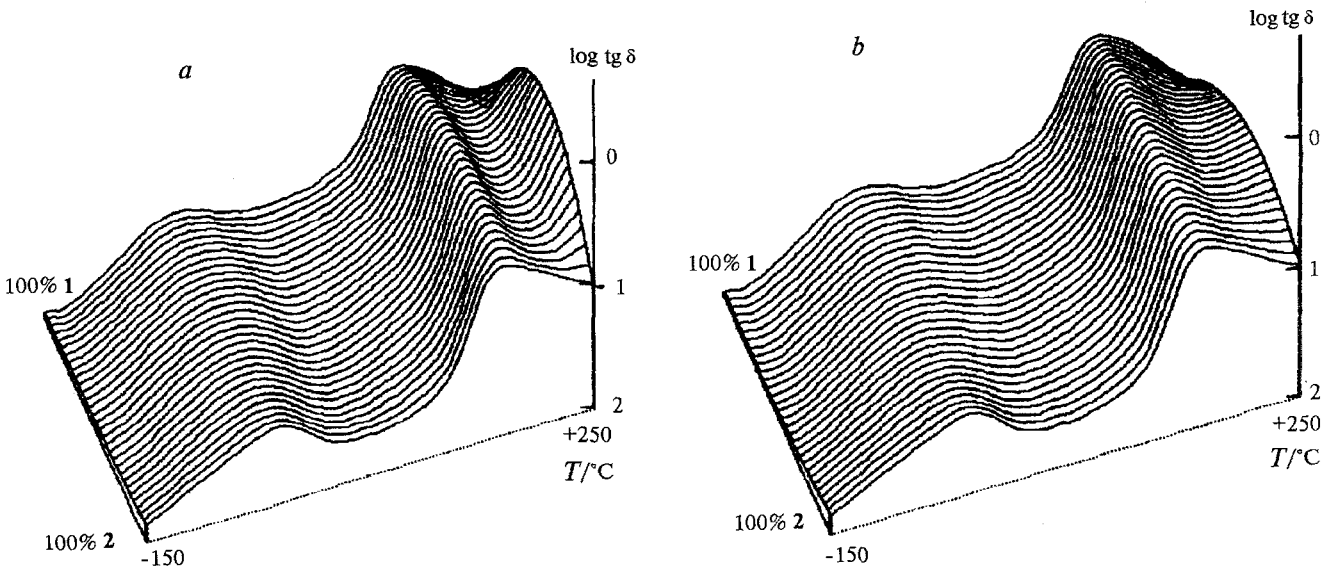

Fig. 16. Dependences of mechanical loss tangent (δ) for copolyesters **1/2** (*a*) and blends of homopoyesters **1** and **2** (*b*).

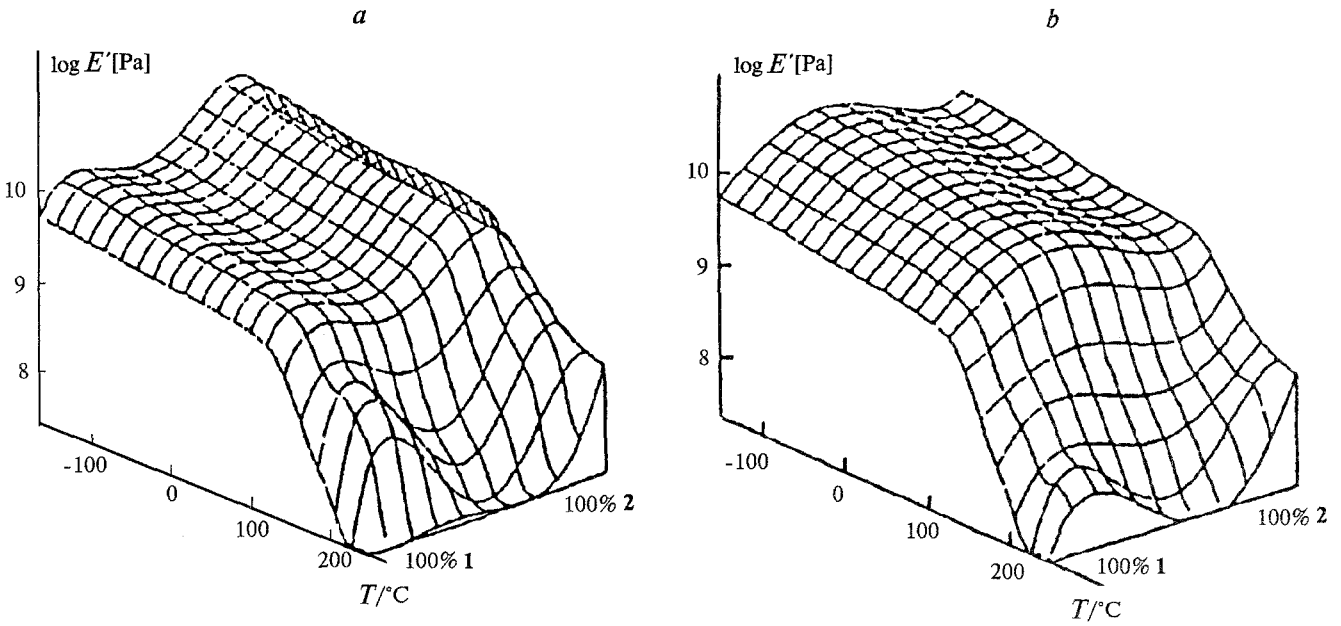

Fig. 17. Temperature—concentration dependences of elastic modulus for copolyesters (*a*) and blend of homopolyesters (*b*).

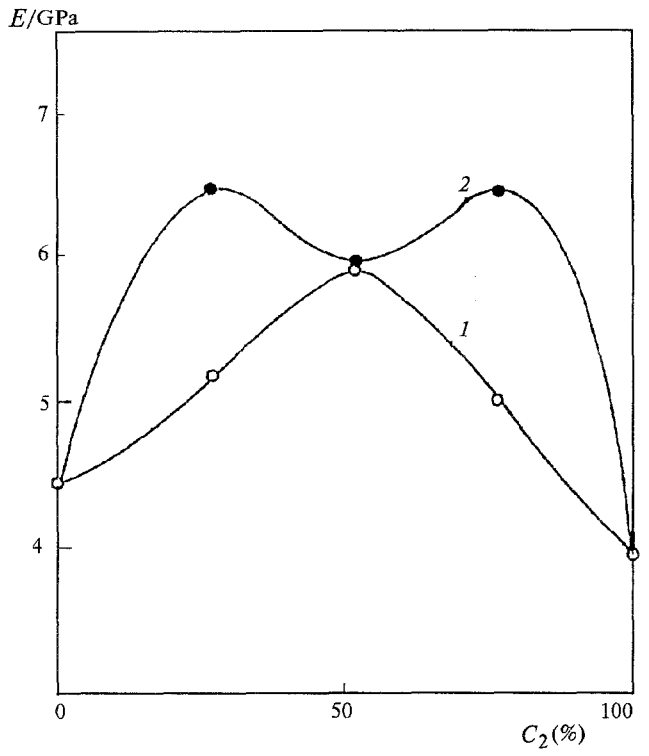

Fig. 18. Concentration dependences of elastic modulus for freshly prepared blends **1** and **2** (*1*) and the same blends after annealing (*2*). C_2, mass fraction of polyester **2**.

corresponding characteristics of random copolymers of terephthalic acid, hydroquinone, phenylterephthalic acid, and phenylhydroquinone[23].

Figure 16 presents the three-dimensional dependences in coordinates of mechanical loss tangent—temperature—composition for the extrudates of mechanical blends and copolyesters. These dependences are essentially similar. This gave us grounds, at a first approximation, to believe that these homopolymers are compatible.

The corresponding dependences for the dymanic elastic modulus are given in Fig. 17. In this case we observe a clear difference in the elastic properties of the mechanical blends and copolyesters. Both systems show bimodal dependence with maxima at 25 and 75% of each component at temperatures above 150 °C, whereas in the case of blends it transforms to unimodal dependence with the maximum at 50% for each copolyester in the region of low temperatures. These data suggest that the rigidity of macromolecules increases as a result of copolycondensation. However, what is the driving force of the synergic effect for mechanical blends?

First, it is not impossible that for the 50:50 blends some incompatibility of the components and reinforcing of one LC polymer with the other is observed. The other reason was found during the study of the effect of annealing (30 min at 350 °C) on the shape of concentration dependences of the static elastic modulus at extension of the blend plates stacked from oriented extrudates (Fig. 18). For the static elastic modulus, the picture is similar to that observed for the dynamic elastic modulus of oriented extrudates: unimodal synergism, although for the 50:50 composition the maximum modulus is not so sharp due to a lesser extent of orientation. Annealing leads to the transformation of the modulus dependence on the blend composition to the bimodal dependence characteristic of copolyesters.

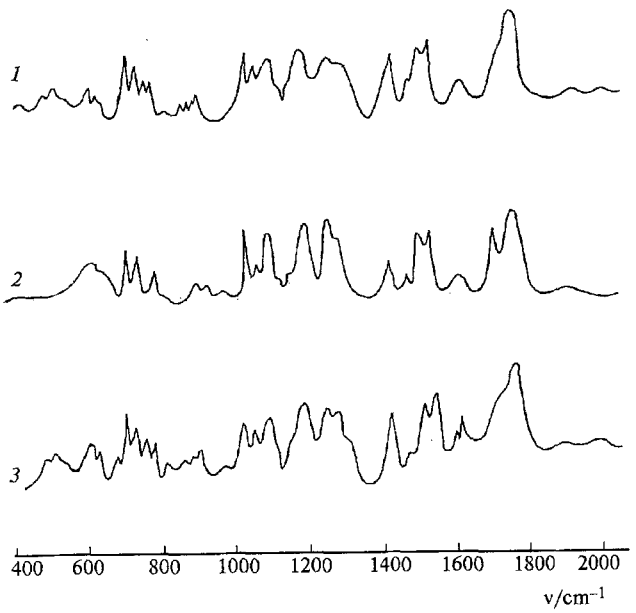

Fig. 19. Portions of IR spectra of copolyester **1/2** (50:50) (*1*), and the freshly prepared blend **1** and **2** (50:50) (*2*), and the same blend after annealing (*3*).

This fact, as well as the coincidence of the shapes of composition dependences of dynamic modulus in the high-temperature region (Fig. 17), clearly indicates the possibility of chemical interaction between the components with partial formation of copolyesters of intermediate composition.

We attempted to follow this process using IR spectroscopy[4]. Figure 19 shows the portions of the IR spectra of copolyester **1/2** (50:50), blends **1** and **2** (50:50) before and after annealing near the melting point of high-melting component. In the 600—800 and 1600—1800 cm^{-1} regions of the spectrum, clear differences are observed for copolyesters and freshly-prepared blends. These differences virtually disappear after thermal treatment of the blends. In our opinion, this fact is evidence that *trans*-esterification occurs in the chains of two homopolymers, thus favoring a change in rigidity and conformation of the copolymer chains. To be sure, the possibility that the chemical interaction of the components begins already during preparation of blends and extrudates and leads to unimodal synergistic effect should not be ruled out.

One more direction of modification of thermoplastics and elastomers, where the role of interphase or adsorption interactions is extremely important, is associated with their filling with disperse material. However, there are practically no published data on filled LC thermoplastics. We shall try to fill this gap with a brief analysis of formation of the interphase layer using as our example a system containing LC copolyester of poly(ethyelene terephthalate) (PETP) with *para*-hydroxybenzoic acid (OBA) as a dispersing medium, and an active conductive filler, carbon black PM-100 as a disperse phase[24,25]. The data on dynamic viscoelastic studies of carbon black-filled compositions are presented in Fig. 20, as conventional temperature—concentration dependences $log\ E'(T,\varphi)$ and $log\ tan\ \delta(T,\varphi)$. The spatial representation of viscoelastic functions provides an idea of the general regularities of mechanical relaxation for the given compositions. In the range of −150...+200 °C, three relaxation regions are observed: low-temperature region I, the major relaxation process II, and high-temperature relaxation III. Process I is associated with the appearance of fragmental mobility of copolyester, and process II is caused by softening of the portions of chains enriched with PETP, whereas process II is connected either with the onset of segmental mobility of the fragments enriched with OBA or the relaxation mobility of local crystallites (junctions) formed by OBA blocks (compositional chemical heterogeneity is typical of this polymer[26]). The filling of LC copolyester with carbon black leads to a change in the intensities of relaxation processes (the height of peaks in Fig. 20, *b* changes). In the region of low filling (2 and 4%) the elastic modulus of the material exceeds the elastic modulus of the other components over the entire temperature interval.

To analyze the evolution of relaxation processes in the filled LC thermoplastics, let us use another procedure, which differs from the method of constructing modulus isolines maps or mechanical loss tangent,

Table 1. Parameters of relaxation processes I—III in carbon black-filled LC copolyester PETP—OBA

Concentration of carbon black	I			II					III		
	$tg\delta_{max}$	T_{max}, °C	U, kJ · mol^{-1}	$tg\delta_{max}$	T_{max}, °C	T_c, °C	B/K	$U(T_c)$, kJ · mol^{-1}	$tg\delta_{max}$	T_{max}	U, kJ · mol^{-1}
0	0.060	−30	13	0.120	73	57	390	133	0.087	128	40
2	0.054	−30	12	0.109	71	57	380	129	0.117	130	40
4	0.051	−30	13	0.112	71	57	380	129	0.106	128	40
10	0.055	−30	13	0.101	71	57	380	129	0.125	128	40
20	0.062	−30	12	0.089	71	57	380	129	0.151	128	40
30	0.052	−30	13	0.070	72	58	350	120	0.167	128	40

namely, the method of separating three superimposing processes I, II, and III. This problem can be solved on the assumption that the model of a standard linear viscoelastic body with discrete spectrum of relaxation times is applicable[27].

According to this model the temperature dependences $E'(T)$, $E''(T)$, and *tan* $\delta(T)$ for the set of n processes can be presented as

$$E' = \sum_{i=1} E_{0i} + \frac{E_{1i}\,\omega^2\tau_i^2(T)}{1+\omega^2\tau_i^2(T)}$$

$$E'' = \sum_{i=1} \frac{E_{1i}\,\omega\tau_i(T)}{1+\omega^2\tau_i^2(T)}$$

$$\text{tg}\,\delta = E''(T)/E'(T)$$

where ω is the cyclic frequency of deformation, E_{0i} and E_{1i} are the elastic constants of the model, and $\tau(T)$ is the temperature dependence of relaxation times for the corresponding process.

The computer simulation showed that the best fit between the model calculations of $E'(T)$ and *tan* $\delta(T)$ is achieved for the functional dependence of relaxation time on temperature when process II is described by the Williams—Landell—Ferry equation, and processes I and III are described by the Arrhenius equation, respectively

$$\tau_1(T) = \tau_{01}\exp\,(U_1/RT) \qquad \text{(I)}$$

$$\tau_2(T) = \tau_{02}\exp\,(B/(T_2 - T)) \qquad \text{(II)}$$

$$\tau_3(T) = \tau_{03}\exp\,(U_3/RT) \qquad \text{(III)}$$

where τ_{0i}, U_i, B and T_2 are the constants, which are determined experimentally.

For each process, the above constants were used to calculate the relaxation parameters (Table 1), where *tan* $\delta_{max,i}$ is the maximum mechanical loss tangent for the particular process, T_{max} is the temperature of loss modulus maximum $E''(T)$ determined for the same process, U_i is the activation energy for processes I and III, and $U(T_g)$ is the apparent activation energy for the main relaxation process at temperature $T_g = -51.6$ (by analogy with determination of the structural glass transition in amorphous polymers).[19]

The Table shows that the introduction of carbon black to copolyester does not essentially affect the temperature characteristics and activation energies of all three processes, although the intensity of the main process II decreases, whereas in process III the mechanical losses sharply increase. The plots illustrating the relative change of *tan* δ with the growth of the content of carbon black in these processes are given in Fig. 21.

If there were no interaction between the surface of the filler and copolyester, the intensity of the main process would decrease linearly with the carbon black concentration and approach to zero at $\phi = 1$ (curve *1*). However, for all the compositions, this dependence is significantly lower (curves *2* and *3*) and, hence, it is suggested that the filler particles play an active role, block or hamper the motion of the particles responsible for this process.

A simple method is proposed for evaluating the thickness of the transition layer or the effective range of the particle field, within which blocking of the kinetic units of a polymer, i.e., the interphase interaction occurs[28]. To do this, it is necessary to know a single

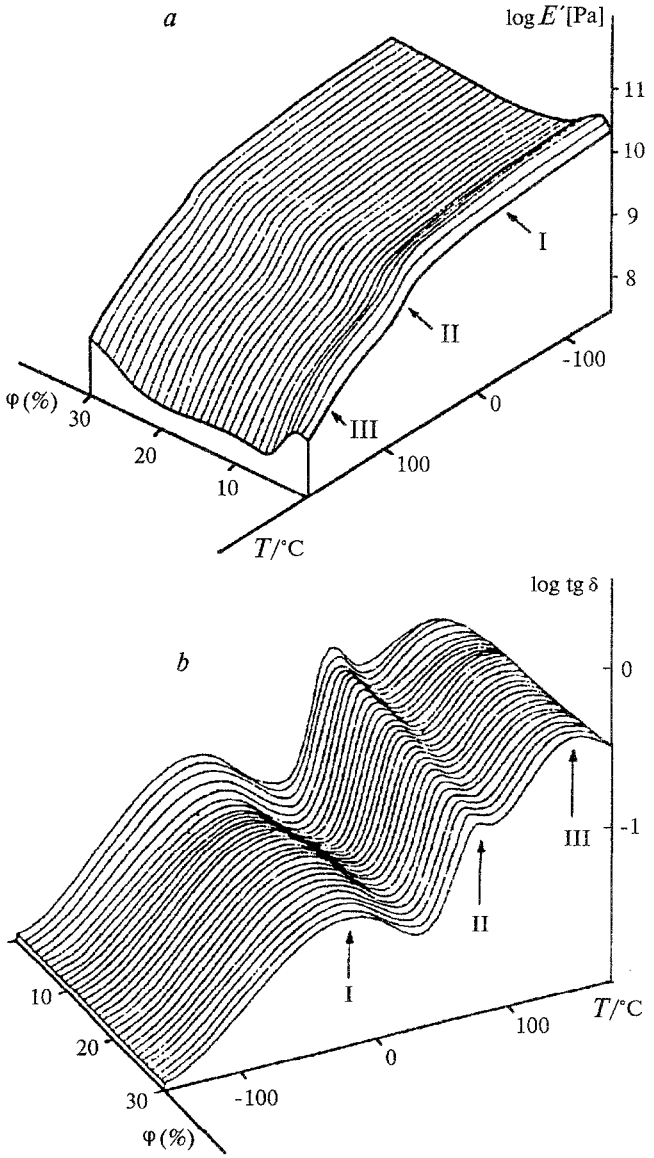

Fig. 20. Dependences of dynamic elasticity modulus (*a*) and loss modulus (*b*) on composition of CPE—carbon black blend and temperature. I, low-temperature region; II, main; and III, high-temperature processes.

parameter — the concentration of a filler $\varphi_{cr}(\phi)$ when the extrapolated dependence *tan* $\delta(\varphi)$ approaches to zero. Then the thickness of the transition layer h can be calculated using the formula

$$h = d\,(\,1/\varphi_{cr} - 1)/2,$$

where d is the diameter of the filler particles. Assuming that the average diameter of the carbon particles is ~30 nm, for process II and a content of carbon black more than 4% we obtain a thickness of the transition layer h_2 = 1.7 nm. The sample containing 2% TC does not fit the above regularity. In the latter case the analogous estimation yields h_3 = 10 nm.

Of particular interest is the fact that for high-temperature relaxation process III, the mechanical loss tangent does not decrease but increases as the concentration of the filler in the system grows, i.e., the number of intermacromolecular contacts increases rather than decreases due to adsorption. On the other hand, judging by the mechanical loss tangent, in relaxation regions II and III the processes may be interrelated.

Let us analyze first process II and compare the effective range of the particle field with the length of mesogenic fragment of macromolecule L. For a given copolyester L = 2.5 nm. In the compositions with the extent of filling more than 0.04 h is equal to 1.7 nm,

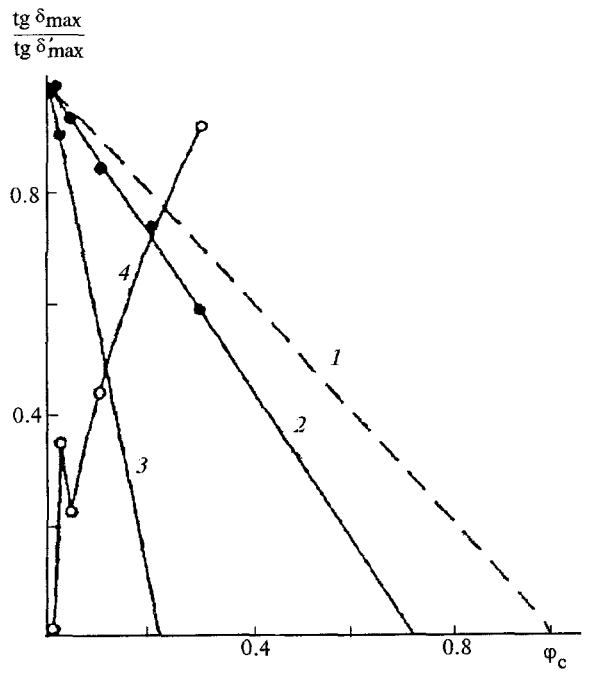

Fig. 21. Dependence of relative mechanical loss tangent on content of filler in (PETP—OBA)—carbon black compositions for processes II (*2*) and III (*4*). *1*) linear approximation of this dependence for inactive filler in the region of process II; *2* and *3*) the same for content of the filler >4% and <2%, respectively. φ_c is the volume fraction of carbon black. δ_{max} and δ'_{max} are the highest values of mechanical loss tangent for the blend and neat copolyester PETP—OBA.

i.e., h is comparable with the length of the mesogenic fragment. Hence, it is apparent that the mesogenic fragment of the macromolecule is the minimum kinetic unit of the main relaxation process, because the process is obviously blocked in filled compositions.

At 2% content of carbon black, the effective size of the particle field is $h = 4L$. In this case, additional slowing down of the segmental mobility accompanied by considerable growth in the elasticity modulus (by 40%) is observed. At low content of the disperse phase, two effects may occur. First, additional orientation of LC matrix under the conditions of convergent (accelerated) flow, when two particles can act like a clamp of a tensile testing machine, stretching anisotropic material between them. Second, due to adsorption and parallelization in an adsorption layer, the filler can effectively increase the rigidity of macromolecules and thus of all the composites. At higher concentrations, agglomeration of carbon black particles may compensate for the effect of reinforcement.

Now let us consider the situation observed in the process of high-temperature relaxation III. Parallelization, i.e., ordering of the stacking of macromolecules in adsorption layers, should favor precrystallization of local sections enriched with units of hydroxybenzoic acid. If it is assumed that in a given polyester this process is initially associated with relaxation of the junctions of the network intermolecular contacts of the crystal nature (this is suggested by the characteristic features of λ-relaxation, namely, the activation energy equal to ~40 kJ/mol independent of the content of the filler), then an increase in the intensity of mechanical losses is caused by an increase in the total density of a network.

Thus, in the PETP—OBA compositions containing LC copolyester, the function of an active disperse filler in the processes of molecular relaxation is to affect the segmental mobility and through this mobility to affect the formation of the supermolecular structure. The structurization of the filler does not directly affect the viscoelastic properties of the composite. Thus, the isolated particles—aggregates transition of particles shows itself indirectly through a decrease in the efficiency of action of the particle force field, whereas the transition associated with the formation of a continuous framework from carbon black particles is not accompanied by any sharp change of viscoelastic functions.

Conclusion

This paper briefly describes some approaches to the study of interphase interactions in heterogeneous polymeric systems containing an LC component. The suggested variant of the method of optical interferometry was first used for nontransparent LC melts. It is extremely useful for evaluating the rate of interdiffusion of compatible pairs of polymers and for constructing phase diagrams.

The method of mechanical spectroscopy provides unique information on the interphase layer in the case of physicochemical interaction of components, and allows one to predict the working capacity of a solidified system. On the other hand, this method is sensitive to the chemical processes occurring in the melts of blends of homopolyesters at high temperature. In this case the formation of copolyesters favors the improvement of mechanical properties, thus opening new possibilities for reaching unique values of elastic modulus, either as a result of copolymerization of three or more comonomers or annealing of the blends of homopolymers.

Therefore, simultaneous study of physical and chemical processes occurring in thermotropic LC polymers at elevated temperatures is a promising direction for further investigations.

For LC polymers filled with disperse materials, the effect of formation of interphase layers also affects the viscous and dissipative mechanical properties. Separation of superimposing relaxation processes and analysis of their evolution under the influence of an active filler allows one to make a justified judgment not only about the blocking of relaxation processes, but about the particular fragments of the chains binding with the surface of filler particles. In the case of polymers prone to crystallization, the filler particles may serve as active centers accelerating the formation of ordered structures.

On the whole, LC thermoplastics are on their way to intensive practical application. Polymer blends and alloys as well as composites are the most probable directions for their industrial application. In this paper we attempted to provide a scientific basis for these applications.

The authors wish to thank O. V. Vasil'eva for the study of dynamic mechanical properties of melts of polysulfone—LC polyester Ultrax blends.

References

1. N. A. Plate' and V. P. Shibaev, *Comb-Shaped Polymers and Liquid Crystals*, Plenum Press, New York-London, 1987.
2. N. A. Plate', V. G. Kulichkhin, and R. V. Talroze, *Pure and Appl. Chem.*, 1991, **63**, 925.
3. *Liquid Crystal Polymers*, Ed. by N. A. Plate', Plenum Press, New York-London, 1993.
4. V. G. Kulichikhin, A. Yu. Bilibin, M. P. Zabugina, and A. V. Semakov, *Processing and Properties of Liquid Crystalline Polymers and LCP Based Blends*, Ed. by D. Acierno, F. LaMantia, Toronto, ChemTec Publ, 1993, p. 89.
5. V. G. Kulichikhin and N. A. Plate', *Vysokomol. Soedin.*, A, 1991, **63**, 3 [*Polym. Sci. USSR, A*, 1991].
6. G. C. Eastmond and S. V. Kotomin, *Polymer*, 1994, **35**, 882.
7. M. Stamm, *Advances in Polymer Science*, 1992, **100**, 357.
8. H. T. Patterson, K. H. Hu, and T. H. Grindstuff, *J. Polym. Sci. : Part C*, 1971, no. **34**, 31.
9. J. J. Elmendorp and G. de Vos, *Polym. Eng. Sci.*, 1986, **26**, 415.
10. A. Cohen and C. J. Carriere, *Rheol. Acta*, 1989, **28**, 223.
11. P. H. M. Elemans, J. M. H. Janssen, and H. E. H. Meijer, *J. Rheol.*, 1990, **34**, 1311.
12. A. E. Chalykh and R. M. Vasenin, *Vysokomol. Soedin., A*, 1966, **8**, 1908 [*Polym. Sci. USSR, A*, 1966, **8**].
13. A. E. Chalykh, *Diffuziya v Polimernykh Sistemakh (Diffusion in Polymeric Systems)*, Khimiya, Moscow, 1987, 312 p.
14. A. E. Chalykh, N. N. Avdeev, A. A. Berlin, and S. M. Mezhikovskii, *Dokl. Akad. Nauk SSSR*, 1978, **238**, 893 [*Dokl. Chem. USSR*, 1978].
15. I. V. Borovskii, K. P. Gurov, and I. D. Marchukova, *Protsessy Vzaimnoi Diffuzii v Splavakh (Processes of Interdiffusion in Alloys)*, Nauka, Moscow, 1973, 359 p.
16. J. Crank, *The Mathematics of Diffusion*, Clarendon Press, Oxford, 1956, 347 p.
17. H. Gramspacher and J. Meissner, *J. Rheol.* (in press).
18. A. V. Semakov, G. Ya. Kantor, O. V. Vasil'eva, I. I. Dobrosol, B. S. Khodyrev, and V. G. Kulichikhin, *Vysokomol. Soedin., A*, 1991, **33**, 161 [*Polym. Sci. USSR, A*, 1991, **33**].
19. V. G. Kulichikhin, O. V. Vasil'eva, I. A. Litvinov, E. M. Antipov, I. L. Parsamyan, and N. A. Plate', *J. Appl. Polym. Sci.*, 1991, **42**, 363.
20. A. V. Semakov, V. G. Kulichikhin, G. Ya. Kantor, E. K. Borisenkova, B. S. Khodyrev, D. R. Tur, and V. G. Kulichikhin, *Vysokomol. Soedin., B*, 1992, **34**, 29 [*Polym. Sci. USSR, B*, 1992, **34**].
21. V. A. Bernshtein, V. M. Egorov, V. A. Marikhin, and L. P. Myasnikova, *Vysokomol. Soedin., A*, 1985, **27**, 771 [*Polym. Sci. USSR, A*, 1985].
22. A. V. Semakov, E. K. Borisenkova, B. S. Khodyrev, D. R. Tur, and V. G. Kulichikhin, *Vysokomol. Soedin., B*, 1989, **31**, 830 [*Polym. Sci. USSR, B*, 1989, **31**].
23. N. A. Plate', V. G. Kulichikhin, and E. M. Antipov, *Vysokomol. Soedin., A*, 1993, **35**, 1743 [*Polymer Science*, 1993, **35**, 1457].
24. V. F. Shumskii, I. P. Getmanchuk, I. L. Parsamyan, Yu. S. Lipatov, and V. G. Kulichikhin, *Vysokomol. Soedin., A*, 1992, **34**, 51 [*Polymer Science, A*, 1992, **34**].
25. V. F. Shumskii, Yu. S. Lipatov, and V. G. Kulichikhin, and I. P. Getmanchuk, *Rheol. Acta*, 1993, **32**, 352.
26. R. S. Benson and D. N. Lewis, *Polym. Commun.*, 1987, **28**, 289.
27. I. M. Ward, *Mechanical Properties of Solid Polymers*, Wiley-Interscience, London-New York-Sydney-Toronto, 1971.
28. A. I. Slutsker, Yu. I. Polikarpov, Yu. N. Fedorov, V. I. Pomerantsev, A. G. Pozamontir, and L. P. Myasnikova, *Vysokomol. Soedin., B*, 1990, 32, 177 [*Polym. Sci. USSR, B*, 1990, **32**].

Received June 6, 1994;
in revised form September 15, 1994